

Quantum Electronic Transport through a Precessing Spin

Jian-Xin Zhu and A. V. Balatsky

Theoretical Division, MS B262, Los Alamos National Laboratory, Los Alamos, New Mexico 87545

The conductance through a local nuclear spin precessing in a magnetic field is studied by using the equations-of-motion approach. The characteristics of the conductance is determined by the tunneling matrix and the position of equilibrium chemical potential. We find that the spin flip coupling between the electrons on the spin site and the leads produces the conductance oscillation. When the spin is precessing in the magnetic field at Larmor frequency (ω_L), the conductance develops the oscillation with the frequency of both ω_L and $2\omega_L$ components, the relative spectrum weight of which can be tuned by the chemical potential and the spin flip coupling.

PACS numbers: 73.63.-b, 75.20.Hr, 73.40.Gk

There has been intensified interest in the electronic transport through atomic impurities or quantum dots in condensed matter physics. The novel features arising from the quantization of both the electronic spectrum and the electronic charge on these impurities have been well studied. More recently, the behavior of a single magnetic spin has also received much attention. The single spin detection and manipulation will play a major role in spintronics and quantum information processing. In spintronics, spins can be used as elementary information storage units [1, 2]. In the realm of quantum computing [3, 4], several architecture proposals rely crucially on the ability to manipulate and detect single spins. So far, the possibility of a single spin observation is a challenging issue. The standard electron spin detection technique - electron spin resonance (ESR) - is limited to a macroscopic number of electron spins - 10^{10} or more [5]. The state-of-the-art magnetic resonance force microscopy has recently achieved the resolution of about 100 fully polarized electron spins [6]. The atomic resolution of the scanning tunneling microscope (STM) can provide an alternative technique for the single spin detection. Manassen *et al.* [7] carried out the STM measurement of the tunneling current while scanning the surface of Si in the vicinity of a local spin impurity (Fe cluster) or imperfection (oxygen vacancy in Si-O) in an external magnetic field. More recently, a similar STM experiment was also performed on organic molecules by Durkan and Welland [8]. Both experiments detected a small signal in the current power at the Larmor frequency. The extreme localization of the signal around the spin site prompted the authors to attribute the detected signal to the Larmor precession of the single spin site. Motivated by Ref. [7], it has been proposed [9] that the spin-orbit interaction of the conduction electrons in the two-dimensional surface may couple the tunneling current to the precessing spin. Instead, the authors of Ref. [10] argued that it is not the spin impurity itself but the current itself that generates the small ac signal. The mechanism for the observed phenomenon is an issue of current debate. In this paper, we address a new spintronic system in which a magnetic spin is weakly coupled to leads. The low-temperature

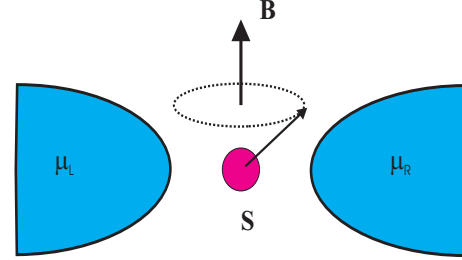


FIG. 1: Magnetic spin coupled to two leads. In the presence of a magnetic field \mathbf{B} , the spin precesses around the field direction.

transport through this magnetic spin is presented by using equations of motion approach. In addition to the interest in its own right, the obtained picture can shed new lights on the mechanism for the above experimental observation.

The model system under consideration is illustrated in Fig. 1. It consists of two ideal leads coupled to a single magnetic spin. In the presence of a magnetic field, the spin precesses around the field direction. We assume that there are no electron-electron interaction and spin-orbit coupling within the metallic leads. The spin-orbit interaction is confined in both barriers between the leads and the single spin site. This experimental setup is different from that studied in Ref. [10], where the single spin in Fig. 1 is replaced by a quantum dot with the spin-degenerate two levels directly split by the magnetic field. We model the spin and its leads by the Hamiltonian:

$$\begin{aligned} \mathcal{H} = & \sum_{k \in (L, R), \sigma} \epsilon_{k\sigma} c_{k\sigma}^\dagger c_{k\sigma} + J \sum_{\sigma, \sigma'} d_\sigma^\dagger \Omega_{\sigma\sigma'} d_{\sigma'} \\ & + \sum_{k \in (L, R), \sigma; \sigma'} (V_{k\sigma, \sigma'} c_{k\sigma}^\dagger d_{\sigma'} + \text{H.c.}) . \end{aligned} \quad (1)$$

Here $c_{k\sigma}^\dagger$ ($c_{k\sigma}$) creates (destroys) an electron with momentum k and spin σ in either the left (L) or the right (R) lead, and d_σ^\dagger (d_σ) is the creation (annihilation) operator of the single electron with spin σ at the magnetic spin site. The quantity $\epsilon_{k\sigma}$ are the single particle energies

of conduction electrons in the two leads. The electrons on the spin impurity site is connected to those in the two leads with the tunneling matrix elements $V_{k\sigma,\sigma'}$. The single electron on the impurity site is coupled to the local spin through a direct exchange interaction of strength J . The form of the coupling matrix $\hat{\Omega}$ in Eq. (1) will be discussed below. Since the Zeeman coupling of the electrons on the impurity site to the external magnetic field is usually very small compared with the exchange coupling to the local spin, this interaction term has been neglected.

The local magnetic spin \mathbf{S} is defined in a three-dimensional spin space. In an external magnetic field \mathbf{B} , a torque will act on the magnetic moment $\boldsymbol{\mu}$ of amount $\boldsymbol{\mu} \times \mathbf{B}$, where $\boldsymbol{\mu} = \gamma \mathbf{S}$ with γ the gyromagnetic ratio. The equation of motion of the local spin is given by $\frac{d\boldsymbol{\mu}}{dt} = \boldsymbol{\mu} \times (\gamma \mathbf{B})$. For a static magnetic field applied along the z direction, we shall see that the local spin would precess about the field in the absence of friction. The coupling matrix then becomes:

$$\hat{\Omega} = \begin{pmatrix} \Omega_{\uparrow\uparrow} & \Omega_{\uparrow\downarrow} \\ \Omega_{\downarrow\uparrow} & \Omega_{\downarrow\downarrow} \end{pmatrix} = \begin{pmatrix} \cos\theta & \sin\theta e^{-i\phi} \\ \sin\theta e^{i\phi} & \cos\theta \end{pmatrix}. \quad (2)$$

In Eq. (2), θ is the angle between $\boldsymbol{\mu}$ and \mathbf{B} , and $\phi = -\omega_L t + \phi_0$ where $\omega_L = \gamma B$ is the Larmor frequency and ϕ_0 is the initial azimuthal angle. If the friction is present between the spin and its environment, the local spin would eventually become parallel to the field. The friction corresponds to the relaxation processes characterized by time T [12]. Therefore, we assume that T is sufficiently long for the precession to be well defined. In the end of the paper, we will make a remark for the case of a finite T .

Since the energy associated with the spin precession, $\hbar\omega_L \sim 10^{-6}$ eV is much smaller than the typical electronic energy on the order of 1 eV, the spin precession is very slow as compared to the time scale of all conduction electron process. This fact allows us to treat the electronic problem adiabatically as if the local spin is static for every instantaneous spin orientation [9]. Our aim is to calculate the conductance through the spin impurity. In a generalized Büttiker-Landauer formalism [11], it can be expressed as [13]:

$$g = \frac{e^2}{h} \int d\epsilon f'_{\text{FD}}(\epsilon) \text{Im}[\text{Tr}\{\frac{2\hat{\Gamma}_L \hat{\Gamma}_R}{\hat{\Gamma}_L + \hat{\Gamma}_R} \hat{G}^r(\epsilon)\}]. \quad (3)$$

Equation (3) expresses the linear-response conductance in terms of the transmission probability weighted by the derivative of the Fermi distribution function, $f'_{\text{FD}} = 1/\{\exp[(\epsilon - \mu)/k_B T] + 1\}$, with μ the chemical potential in the equilibrium state. The transmission probability is constructed as a product of the elastic coupling to the leads and the Green function of electrons on the spin impurity site. The coupling to the leads is represented by

the full line-width function:

$$\Gamma_{\sigma\sigma'}^{L(R)} = 2\pi \sum_{k,\sigma'' \in L(R)} V_{k,\sigma'';\sigma}^* V_{k,\sigma'';\sigma'} \delta(\epsilon - \epsilon_k). \quad (4)$$

Here we have assumed that the couplings to the left and right leads are factorizable, i.e., $\hat{\Gamma}^L = \lambda \hat{\Gamma}^R$ [13]. The quantity in Eq. (3) $\hat{G}^r(\epsilon)$ is the Fourier transform of the retarded Green function for electrons on the spin impurity site:

$$G_{\sigma\sigma'} = -i\Theta(t)\langle [d_\sigma(t), d_{\sigma'}^\dagger(0)]_+ \rangle, \quad (5)$$

where $[\dots]_+$ denotes the anticommutator, $\Theta(t)$ is the Heaviside step function, and $d_\sigma^\dagger(t)$ ($d_\sigma(t)$) are the impurity-site electron operators in the Heisenberg picture, e.g., $d_\sigma(t) = e^{iHt} d_\sigma e^{-iHt}$. Note that both $\hat{\Gamma}$ and \hat{G}^r are matrices in the spin space of the impurity-site electron.

The remaining task is to evaluate the impurity-site electron Green function. This calculation should be done in the presence of the coupling to leads. We employ the equations-of-motion method to this end. It consists of differentiating $G_{\sigma\sigma'}$ with respect to time, thereby generating new Green functions. As we will show below, in the absence of electron correlation, the equations of motion for $G_{\sigma\sigma'}$ can be closed exactly. Otherwise, the higher-order equations-of-motion arising from electron correlation must be truncated to close the equations-of-motion for $G_{\sigma\sigma'}$. Using the commutator $[d_\sigma, H]_-$, we find the equation of motion for $G_{\sigma\sigma'}$:

$$i \frac{\partial G_{\sigma\sigma'}(t)}{\partial t} = \delta(t) \delta_{\sigma\sigma'} + J \sum_{\sigma''} \Omega_{\sigma\sigma''} G_{\sigma''\sigma'}(t) + \sum_{k,\sigma'' \in L(R)} V_{k,\sigma'';\sigma}^* G_{k\sigma'',\sigma'}(t). \quad (6)$$

The time derivative of $G_{\sigma\sigma'}$ generates a new Green function:

$$G_{k\sigma,\sigma'} = -i\Theta(t)\langle [c_{k\sigma}(t), d_{\sigma'}^\dagger(0)]_+ \rangle, \quad (7)$$

which is originated from the coupling of the impurity-site electron to the leads. Using the commutator $[c_{k\sigma}, H]_-$, we can also obtain:

$$i \frac{\partial G_{k\sigma,\sigma'}(t)}{\partial t} = \epsilon_k G_{k\sigma,\sigma'}(t) + \sum_{\sigma''} V_{k,\sigma'';\sigma} G_{\sigma''\sigma'}(t). \quad (8)$$

Equation for $G_{k\sigma,\sigma'}$ (6) now closes with the aid of Eq. (8). Performing the Fourier transform of these Green functions, we obtain Eqs. (6) and (8) in the frequency space:

$$\omega G_{\sigma\sigma'}(\omega) = \delta_{\sigma\sigma'} + J \sum_{\sigma''} \Omega_{\sigma\sigma''} G_{\sigma''\sigma'}(\omega) + \sum_{k,\sigma'' \in L(R)} V_{k,\sigma'';\sigma}^* G_{k\sigma'',\sigma'}(\omega), \quad (9)$$

and

$$\omega G_{k\sigma,\sigma'}(\omega) = \epsilon_k G_{k\sigma,\sigma'}(\omega) + \sum_{\sigma''} V_{k\sigma,\sigma''} G_{\sigma''\sigma'}(\omega). \quad (10)$$

A little algebra yields the solution:

$$G_{++}(\omega) = \frac{1}{\omega - (J\Omega_{++} + \Sigma_{++}) - \Sigma_1}, \quad (11a)$$

$$G_{+-}(\omega) = \frac{(J\Omega_{+-} + \Sigma_{+-})G_{--}(\omega)}{\omega - (J\Omega_{++} + \Sigma_{++})}, \quad (11b)$$

$$G_{-+}(\omega) = \frac{(J\Omega_{-+} + \Sigma_{-+})G_{++}(\omega)}{\omega - (J\Omega_{--} + \Sigma_{--})}, \quad (11c)$$

$$G_{--}(\omega) = \frac{1}{\omega - (J\Omega_{--} + \Sigma_{--}) - \Sigma_2}. \quad (11d)$$

In Eq. (11), the self-energy matrix due to the coupling to the leads is:

$$\Sigma_{\sigma\sigma'}(\omega) = \sum_{k,\sigma'' \in L,R} \frac{V_{k\sigma'',\sigma}^* V_{k\sigma'',\sigma'}}{\omega - \epsilon_k}, \quad (12)$$

and

$$\Sigma_1(\omega) = \frac{(J\Omega_{+-} + \Sigma_{+-})(J\Omega_{-+} + \Sigma_{-+})}{\omega - (J\Omega_{--} + \Sigma_{--})}, \quad (13)$$

$$\Sigma_2(\omega) = \frac{(J\Omega_{-+} + \Sigma_{-+})(J\Omega_{+-} + \Sigma_{+-})}{\omega - (J\Omega_{++} + \Sigma_{++})}. \quad (14)$$

Equation (12) shows that the structure of the self energy is determined by the nature of the tunneling matrix elements $V_{k\sigma,\sigma'}$. The retarded self energy can be written in terms of the principle and imaginary parts:

$$\begin{aligned} \Sigma_{\sigma\sigma'}^r(\omega) &= \mathcal{P} \sum_{k,\sigma'' \in L,R} \frac{V_{k\sigma'',\sigma}^* V_{k\sigma'',\sigma'}}{\omega - \epsilon_k} \\ &\quad - \frac{i}{2} [\Gamma_{\sigma\sigma'}^L(\omega) + \Gamma_{\sigma\sigma'}^R(\omega)], \end{aligned} \quad (15)$$

where the full line-width functions have been given by Eq. (4). The solution for $\hat{G}^r(\omega)$, as given by Eq. (11), can now be employed to evaluate the conductance by Eq. (3). The structure of the full line-width functions, $\hat{\Gamma}^{L,R}$, is determined by the details of the tunneling matrix $V_{k\sigma,\sigma'}$. We use the full line-width functions as the coupling parameters. The full retarded self-energies $\hat{\Sigma}^r$ are evaluated according to Eq. (15). For simplicity, we assume symmetric tunneling barriers between the local spin and the leads, therefore, $\hat{\Gamma}^L = \hat{\Gamma}^R = \hat{\Gamma}$. Since the density of states around the Fermi surface in the leads are broad and flat, the couplings are constant. In the following analysis, we measure the energy in units of the exchange integral between the electrons and the local spin, J , and consider the conductance at zero temperature. In zero magnetic field, the spin is static. In Fig. 2, we plot the conductance versus the chemical potential with various values of the spin-flip coupling $\Gamma_{+-} = \Gamma_{-+} = \Gamma_s$.

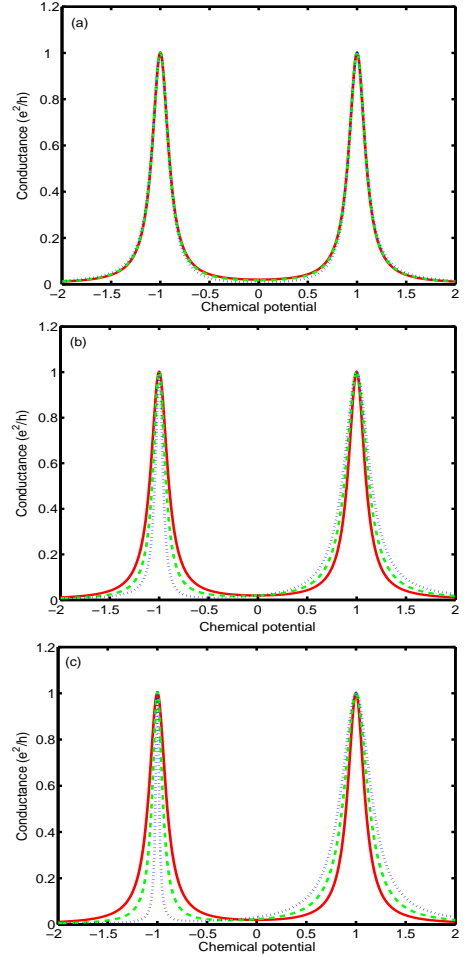


FIG. 2: Conductance versus the chemical potential μ with various values of the spin-flip coupling $\Gamma_s/\Gamma_n = 0.0$ (red-solid line), 0.4 (green-dashed line), and 0.8 (blue-dotted line). The results shown in panels (a) through (c) correspond to three different local spin orientations in zero magnetic field: $(\theta, \phi_0) = (0, 0)$, $(\pi/4, 0)$, $(\pi/2, 0)$. The spin-conserved coupling, $\Gamma_n = 0.1$.

The results shown in panels (a)-(c) correspond to the three different spin orientations: $(\theta, \phi_0) = (0, 0)$, $(\pi/4, 0)$, $(\pi/2, 0)$. The spin-conserved couplings are taken to be $\Gamma_{++} = \Gamma_{--} = \Gamma_n = 0.1$. From Fig. 2, the generic feature of the conductance as a function of the chemical potential is: As μ passes through ± 1 , the conductance exhibits the resonant behavior by showing a peak at these energy position. The resonant level position is independent of the local-spin orientation. The spin-flip couplings does not change the resonant level position either. However, they change the line-width of the resonant peaks. Explicitly, with the increasing spin-flip couplings, the resonant peak at -1 is narrowing while that at $+1$ is broadening, but both with the maximum peak intensity almost unchanged.

As we have shown, in the presence of magnetic field, the local spin will precess with the Larmor frequency.

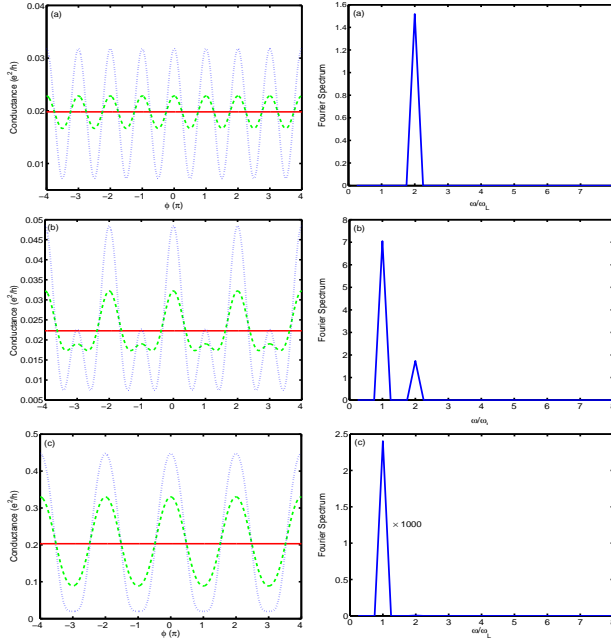


FIG. 3: Conductance versus the phase ϕ accumulated by the precession of the local spin with various values of the spin-flip coupling $\Gamma_s/\Gamma_n = 0.0$ (red-solid line), 0.4 (green-dashed line), and 0.8 (blue-dotted line). The results shown in the left panels (a) through (c) correspond to three different values of the chemical potential: $\mu = 0, 0.4$, and 0.8 . Also shown in the right panels is the Fourier spectrum for $\Gamma_s/\Gamma_n = 0.4$ with the chemical potential same as in the left panels. Other parameter values: $\Gamma_n = 0.1$, $\theta = \pi/2$, and $\phi_0 = 0$.

The question is whether this Larmor precession will manifest in the conductance of electrons transported through this local spin, which we now address below. To be relevant to the experimental situation, we consider the electron tunneling in the off-resonance regime by choosing the value of the chemical potential other than ± 1 . In Fig. 3, we plot the conductance as a function of the phase ϕ accumulated by the precession of the local spin for various values of the spin-flip couplings. Without loss of generality, we have taken $\theta = \pi/2$ and $\phi_0 = 0$. The results shown in the left panels (a)-(c) correspond to three typical values of the chemical potential $\mu=0, 0.4$, and 0.8 . Also shown in the right panels is the Fourier spectrum for a fixed value $\Gamma_s/\Gamma_n = 0.4$ with the chemical potential same as in the left panels. Several features are noteworthy: (i) The conductance oscillation occurs only when the spin-flip couplings is nonzero and its oscillation amplitude increases with the spin-flip couplings. (ii) When $\mu = 0$, the conductance exhibits the periodicity of π (see Fig. 3(a)), which corresponds to the oscillation of frequency $2\omega_L$. When μ is nonzero, the conductance oscillates in phase with a basis period of 2π , that is, with frequency ω_L (see Fig. 3(b) and (c)). Generally, there still exists of the $2\omega_L$ mode, the Fourier spectral weight of which decreases with the deviation of μ from

zero but is enhanced by the spin-flip couplings. These modes can be seen more clearly from the Fourier spectrum. Analytically, we find that the imaginary part of the off-diagonal components of the retarded Green function satisfy $\text{Im}G_{+-}^r(\phi + \pi) = \text{Im}G_{-+}^r(\phi)$. Therefore, $\text{Im}[G_{+-}^r + G_{-+}^r]$ is a periodic function of ϕ with a period of π . However, the periodicity of $\text{Im}G_{++}^r$ and $\text{Im}G_{--}^r$ depends on the position of the chemical potential. With a little algebra, one can obtain:

$$\text{Im}[G_{++}^r + G_{--}^r] = \frac{-4\omega(J \sin \theta \Gamma_s \cos \phi + \omega \Gamma_n) + 2\Gamma_n \tilde{\omega}^2}{\tilde{\omega}^4 + 4(J \sin \theta \Gamma_s \cos \phi + \omega \Gamma_n)^2}, \quad (16)$$

and $\tilde{\omega} = [\omega^2 - J^2 - \Gamma_n^2 + \Gamma_s^2]^{1/2}$. Equation (16) shows that the contribution to the conductance from the spin-conserved couplings involves the linear term and quadratic term in $\cos \phi$. When $\omega = 0$, the linear term vanishes, and the oscillation is determined solely by the $\cos^2 \phi$ term. This explains why the conductance oscillates with frequency $2\omega_L$ as $\mu = 0$. Moreover, since the contributions to the conductance from $\text{Im}[G_{++}^r + G_{--}^r]$ and $\text{Im}[G_{+-}^r + G_{-+}^r]$ are weighted by Γ_n and Γ_s , respectively, one can expect that the spectral weight of $2\omega_L$ mode in the conductance oscillation is appreciable for a large ratio of Γ_s/Γ_n even when $\mu \neq 0$.

To conclude, we have studied the quantum transport through a local impurity spin precessing in an external static magnetic field. We have found that the spin-flip coupling between the conduction electrons on the spin and those in the leads are crucial to the appearance of the conductance oscillation. We have also predicted that there exists the oscillation mode with frequency *twice of the Larmor frequency*, the Fourier spectral weight of which can be tuned by the position of the chemical potential and spin flip coupling.

The following remarks are in order: We have assumed that the dynamics of the local spin is controlled by the magnetic field only and no decoherence mechanism is included, and have concentrated on the forward action of the spin on the transport properties of conduction electrons. In reality, the dynamics of the local spin is also influenced by the backaction of the transport currents due to its coupling to the conduction electrons. Therefore, our results should be valid in the weak measurement regime, where the spin relaxation time is sufficiently long. In the opposite regime, the interactions of the spin with its surroundings are so strong that the spin precession will die out quickly and the spin is aligned with the magnetic field \mathbf{B} . One then can apply a small r.f. field perpendicular to the static magnetic field. By solving the Bloch equation, one can find the transverse components of the spin oscillate with the r.f. frequency. This leads to an exchange interaction between a driven spin and conduction electrons very similar to that given by Eq. (2). Therefore, the conductance can be evaluated by following

the same procedure and the conclusion about the conductance oscillation remains. This setup is experimentally accessible, the measurement from which will provide an additional test of the proposed mechanism for the conductance oscillation.

Note Added: While working on this paper, we became aware of earlier work by Aronov and Lyanda-Geller [14], where the oscillation of average electron spin at the frequency of an alternating electric field was shown.

Acknowledgments: The authors thank Y. Manassen, Y. Meir, D. Mozyrsky, and B. Spivak for helpful discussions. This work was supported by the Department of Energy through the Los Alamos National Laboratory.

-
- [1] G. Prinz, *Science* **282**, 1660 (1998).
 - [2] S. A. Wolf *et al.*, *Science* **294**, 1488 (2001).
 - [3] B. E. Kane, *Nature* **393**, 133 (1998).
 - [4] D. Loss and D. P. DiVincenzo, *Phys. Rev. A* **57**, 120

- (1998).
- [5] M. Farle, *Rep. Prog. Phys.* **61**, 755 (1998).
- [6] K. J. Bruland *et al.*, *Appl. Phys. Lett.* **73**, 3159 (1998).
- [7] Y. Manassen, I. Mukhopadhyay, and N. Ramesh Rao, *Phys. Rev. B* **61**, 16223 (2000); Y. Manassen, R. J. Hamers, J. E. Demuth, and A. J. Castellano, Jr., *Phys. Rev. Lett.* **62**, 2531 (1989); D. Shachal and Y. Manassen, *Phys. Rev. B* **46**, 4795 (1992); Y. Manassen, *J. Magnetic Reson.* **126**, 133 (1997).
- [8] C. Durkan and M. E. Welland, *Appl. Phys. Lett.* **80**, 458 (2002).
- [9] A. V. Balatsky and I. Martin, cond-mat/0112407.
- [10] D. Mozyrsky *et al.*, cond-mat/0201325.
- [11] M. Büttiker, *Phys. Rev. Lett.* **57**, 1761 (1986); R. Landauer, *Philos. Mag.* **21**, 863 (1970).
- [12] Here we do not address the difference between the longitudinal (T_1) and transversal (T_2) relaxation time since these times are defined for ensemble not single spins.
- [13] Y. Meir and N. S. Wingreen, *Phys. Rev. Lett.* **68**, 2512 (1992).
- [14] A. G. Aronov and Yu. B. Lyanda-Geller, *Pis'ma Zh. Eksp. Teor. Fiz.* **50**, 398 (1989).